Aspects on the shape dependence with energy of point-like events in high resistivity CCDs

Guillermo Fernndez Moroni*, Miguel Sofo Haro†, Javier Tiffenberg‡, Eduardo Paolini §, Juan Estrada‡, Xavier Bertou † and Gustavo Cancelo‡

*Instituto de Inv. en Ing. Eléctrica, Dept. de Ingeniería Eléctrica y de Computadoras, Dept. de Matemática, Universidad Nacional del Sur (UNS)-CONICET, Bahía Blanca, Argentina.

† Centro Atómico Bariloche Instituto Balseiro, CNEA/CONICET, Argentina

‡Fermi National Accelerator Laboratory, Batavia, IL, U.S.A.

§ Comisión de Investigaciones Científicas, Provincia Buenos Aires, La Plata, Argentina

¶ Instituto de Inv. en Ing. Eléctrica, Dept. de Ingeniería Eléctrica y de Computadoras, Universidad Nacional del Sur (UNS)-CONICET, Bahía Blanca, Argentina.

***Abstract*—Fully depleted thick CCDs have been designed for infrared astronomy, but their low read-out noise of the order of approximately $2\,\mathrm{e}^-$ and their considerable mass of approximately $5.2\,$gr, allows novel uses for them in low energy threshold particle detection applications, such as the CONNIE and DAMIC experiments. In both experiments, the neutrinos or WIMPS will generate e-h pairs in a volume much less than the pixel size, they will produce events like points in the output image, of less than 10 pixels. Is well understood that one of the factors that define the size of the events is the diffusion process. In this work we will demonstrate with experimental results and through simulation, that there is also a dependence of the size with the amount of charge generated by the event, due to charge repulsion effects.**

***Index Terms*—CCD, X-rays, charge repulsion, point-like events**

I. Introduction

Although invented as memory devices [1], [2], Charge Coupled Devices (CCDs) have found a niche as imaging detectors due to their ability to obtain high resolution digital images of objects placed in its line of sight. In particular, scientific CCDs have been extensively used in ground and space-based astronomy and X-ray imaging [3]. CCDs have high detection efficiency, low noise, good spatial resolution, and low dark current. Furthermore CCDs can be made thick to increase their detector mass, enabling their use as particle detectors [4]. In particular, their extremely low read-out noise around $2\,\mathrm{e}^-$ makes observations with a low energy threshold of $50\,$eVee possible [5].

Two novel experiments take advantage of this technology to detect the interactions between incoming particles and a nucleus of the silicon atoms of the CCD. One is the direct dark matter detector called DAMIC (Dark matter in CCDs) [5]; the other one is the CONNIE experiment (Coherent Neutrino-Nucleus Interaction Experiment) [6] which aims at the detection of the neutrino-nucleus coherent scattering interaction, which is predicted but has yet to be observed.

The detection principle of both experiments is similar and it is as follows, the neutrino or WIMP will collide with a Si nucleus, and then, its recoil will produce e-h pairs, the holes are drifted by the electric field in the CCD bulk and collected in the potential well of the pixels. The expected recoil energy is below 1 keV [6], hence the nucleus range will be < 2 μm, producing all the e-h pairs in a small volume compared to the pixel size ($15{\times}15\mu m$), we call this point-event. The events will have less than $100e^-$ because only a fraction of the recoil energy is converted in e-h pairs [7].

In both systems the spurious events from background particles limits the detection. The implementation of an active background rejection veto is difficult due to the long readout times of the detectors. More details about veto rejection in the context of a neutrino experiment can be found in [8]. DAMIC and CONNIE only use passive shield to reduce these events.

Other particles like low energy photons, gammas, electrons and neutrons also produce points-like events and constitute the background signal for the experiments. In particular, low energy photons and electrons have a large cross section in silicon, and therefore their deposition of energy will be placed in the first few microns from the surfaces of CCD. In the other hand, Dark Matter and Neutrinos are expected to interact at any depth with equal probability. Hence, the rejecting of events in the first and last few microns of the CCD will improve the signal-to-background ratio of the detection.

A proper understanding of point-events is very important because measuring its size in the images is possible to estimate its depth in the bulk and apply depth cuts to improve the signal-to-background ratio[5].

In section II a description of the used CCD is presented. In section III an overview of point like and how they spread in the images is described. Experimental results exposing the CCD to different X-rays energies is detailed in section IV. Section V shows simulations matching the experimental results. Finally, some final comments are presented in section VI.

II. Fully Depleted Thick CCDs

The structure of a scientific CCD developed by Lawrence Berkeley Laboratory, and extensively characterized at Fermilab for the DECam project [4], [9] is shown in Fig. 1. Several

978-1-5090-5859-4/17/$31.00

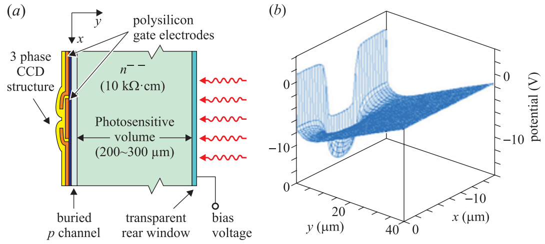

Fig. 1. Pixel-cross section of a 250 μm thick CCD developed by Lawrence Berkeley Laboratory. The electrostatic potential generated by the three phases under the gates is also shown as a function of depth (Y axis) and one of the lateral directions (X axis).

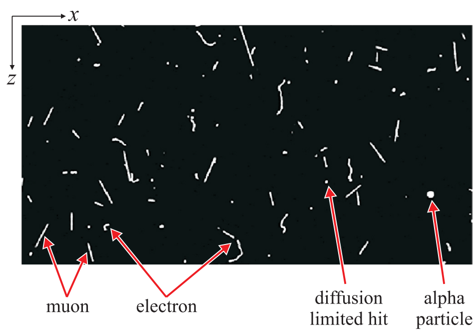

Fig. 2. Compendium of particle events at sea level using a 250 μm CCD.

million pixel CCD are fabricated on high resistivity silicon to maximize the depleted silicon volume and therefore increase the near-IR photon response. The thickness of these detectors is 250 μm, with a mass of approximately 1 gram. The CCDs are fully depleted using a substrate voltage. The CCDs are three-phase, p-channel, back illuminated with a special coating in the backside to increase photon absorption and to reduce back side dark current generation. However, for neutrino detection the optical features are not relevant. Pixel size is 15 μm$\times$ 15 μm. This small size gives very good spatial resolution that can be efficiently used in these rare events experiments to reject some of the background interactions.

A compendium of backgrounds events from blind measurements at sea level is shown inf Fig. 2: muon tracks appear as a straight line crossing the entire silicon volume; energetic electrons from electromagnetic radiation produce wiggling tracks called worms; bright large dots are produced by alpha particles as a consequence of the plasma effect that they generate in the silicon [10]. Point like events, expected from the coherent neutrino-nucleus scattering and dark matter interaction, appear as energy deposition within a single pixel volume where some of the ionized charge flows to neighbor pixels by diffusion and as we present in this work by charge repulsion effects.

III. Point like events

In spite of the charge is generated in a volume less that the pixel size, it is spread over several pixels. This effect is attributed to the diffusion of the charge while it is drifted to the pixel collection well[11], [6]. If only diffusion is considered, the size of events only depends on the thermal energy of the material and the time free carriers have before being trapped by the collection Well[5], [11], and it should not be related with the charge generated by the event.

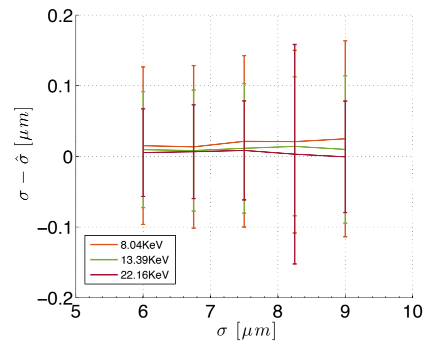

Fig. 3. Errors of the MLE of σ

The diffusion of the X-ray events should be measured from the pattern of the event in the output image. For this procedure we use a maximum likelihood algorithm using an approximation of the probability density function of point events presented in [11]. The approximation assumes that the charge of the different pixels that form the event is not correlated among them, so the calculation of the multinomial distribution can be simplified to the product of individual binomial distributions. The probability density function is

$$f_{\mathbf{P}}(\mathbf{p}; Q_T, x_g, z_g, \sigma_D) = \prod_{i=1}^{N_p} \sum_{q_i=0}^{Q_T} \frac{Q_T! \lambda_i^{q_i} (1-\lambda_i)^{Q_T - q_i}}{q_i!(Q_T - q_i)!} \frac{e^{-\frac{(p_i - q_i)^2}{2\sigma_R^2}}}{\sigma_R \sqrt{2\pi}} \quad (1)$$

where $\mathbf{P} = (P_1, ..., P_{N_p})^T$ is the vector of random variables of the pixels value of the event, Q_T is the total charge of the event, σ_R is the standard deviation of the readout noise explained above, N_p is the number of pixels in the events, and (x_g, y_g, z_g) are the coordinates in the volume of the detector where the charge was generated, σ_D is the diffusion of the event, and λ_i is the probability that one electron generated by the X-rays ends in the pixel i given by

$$\lambda_i = \int_{x_{i,o}}^{x_{i,f}} \int_{z_{i,o}}^{z_{i,f}} \frac{e^{-[(x-x_g)^2 + (z-z_g)]^2/(2\sigma_D^2)}}{2\pi\sigma_D^2} dz dx. \quad (2)$$

Then the σ_D is obtained by maximizing the function $f_{\mathbf{P}}(\mathbf{p}; Q_T, x_g, z_g, \sigma_D)$ for each set of pixels ($\mathbf{p}$)

$$L(Q_T, x_g, z_g, \sigma_D) = \frac{max}{Q_T, x_g, z_g, \sigma_D} f_{\mathbf{P}}(\mathbf{p}; Q_T, x_g, z_g, \sigma_D). \quad (3)$$

Events with the energy of copper (Cu), lead (Pb) and silver (Ag) K_α X-rays fluorescence peak had been simulated with different σ to study the errors of the estimator after using the event clustering method, the results in figure 3 shows that the MLE (Maximum Likelihood Estimation) do not introduce a bias with the energy, and the error is less than 0.2μm

IV. Experimental results

The CCDs used in both experiments have 8M pixels of 15μm $\times$15μ with a thickness of 250μm. The devise has an

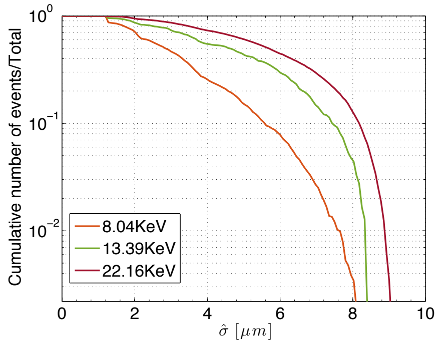

Fig. 4. Measured cluster diffusion as a function of the energy of the event.

active mass of $\approx$ 1.1 grams and covers an area of approximately 6 by 3 cm. In both experiences the CCDs are cooled at -150^oC to avoid any dark current generation. They are used in fully depleted operation with a substrate voltage of 40 V [12]. The device is glued from the back side to an aluminum nitride (AlN) plate which provides mechanical support and thermal conductivity. The CCD is placed inside a prove vessel with a radioactive source. The measured readout noise of the system was 2 e^-.

The CCD were exposed to collimated X-rays, with an angle less than 3°, from the fluorescence of Cu, Pb and Ag. The plot in figure 4 is the cumulative distribution of the σ parameter for the three different X-rays energies. For each X-ray the maximum spread ($\hat{\sigma}_{MAX}$) is different, showing a dependence of σ with the amount of charge generated by the X-ray. This effect observed and characterized for silicon drift detectors (SDD) [13], [14] and pnCCD [15], it is due to charge repulsion and the size of the primary charge cloud formed by the X-rays.

Figure 5 also shows this behavior. The spatial standard deviation and energy of each event is depicted with blue dots in the figure. At this time the CCD is exposed to a Molybdenum X-ray source The dense cloud of points with size around 0.5 pixels at all energies correspond to events interacting at the back edge of the detector, mainly free electrons produced in the surrounding materials that reach the detector. A clear increasing tendency with energy is observed. The vertical lines correspond to the X-rays peaks from the source and from fluorescence in materials facing the detector. The horizontal lines for low event sizes correspond to events reaching the detector from the front side. Higher errors in the reconstruction of size are expected in this region since all the charge information is almost carried by a single pixel.

V. Simulation

Simulation of point like events were used to understand the change on the cluster size as a function of its energy.

1) Algorithm: The final standard deviation of the shape of events produced by low energy photons and electrons can be understood by three mechanisms:

- Ionization-track length of the primary electron. This electron can be produced either in the silicon volume by the interaction of an incoming photon or in the surrounding materials. This track will be the original position of the free carriers.
- Diffusion of free carriers in silicon.
- Repulsion of free carriers.

The developed algorithm follows the ideas presented in [16] for simulating of the cluster size of alpha particles interacting with silicon. It is based on the transport of free charge in a silicon volume affected by a constant electric field that attracts hole to the pixel potential Well. In our simulation, the first mechanism accounting the range of the primary electron has been also incorporated. The algorithm flow can be summarized in the following steps:

1) The first step of the simulation is to find the initial position of the free charge. This condition is calculated using the range of the ionizing electron, which is a function of its energy [17]: $R_{e^-} = 0.0171 E_{e^-}$, where E_{e^-} is the energy of the ionizing electron in keV and R_{e^-} is its range. The generated initial electron cloud is assumed to have a spherical shape with a Gaussian profile with a standard deviation (σ_{init}) [18]: $\sigma_{init} = 0.257 R_{e^-}$.
2) The second part of the simulation is loop over time in steps of Δt seconds until all the charge reaches the position of the potential well of the pixels in the array. At this point the charges are no longer used for the transport calculations. On each cycle different variables are calculated:
   - The total electric field applied to each charge ($\vec{E}_{tot}$) by the other free carriers is computed.
   - The next step si to get the drift mobility coefficient of each carrier [19]:

$$\mu = \frac{\mu_0}{\left(1 + \left(\frac{\mu_0 E_{tot}}{v_{sat}}\right)^{\beta}\right)^{\frac{1}{\beta}}}$$

   where μ_0 = 2300 $cm^2/(Vs)$ is the intrinsic mobility of holes in silicon at a temperature of 140K [20], E_{tot} is the magnitude of the calculated electric field $\vec{E}_{tot}$, β is a constant ($beta$=2 for holes, $beta$=1 for electrons), and v_{sat} is the saturation velocity of holes in silicon calculated as [21]

$$v_{sat}\left(\frac{cm}{s}\right) = \frac{2.45 \times 10^7}{1 + 0.8^{\frac{T(K)}{600}}}$$

   .

   - The velocity of each carrier ($\vec{v}_{elec}$) produced by the electromagnetic interaction is:$\vec{v}_{elec} = \mu \vec{E}_{tot}$.
   - Then, the change in the position by this process (Δs_{elec}) is calculated using $\Delta s_{elec} = \Delta t \vec{v}_{elec}$
   - A displacement by diffusion process of the free carriers in the silicon net is calculated using $\Delta s_{diff} = \sqrt{2D}\Delta t$.
   - The new position ($\vec{s}_{i+1}$) for the next iteration ($i+1$) is calculated as the sum of both displacements from the initial position ($\vec{s}_i$) of the current cycle

$$\vec{s}_{i+1} = \vec{s}_i + \Delta s_{elec} + \Delta s_{diff}$$

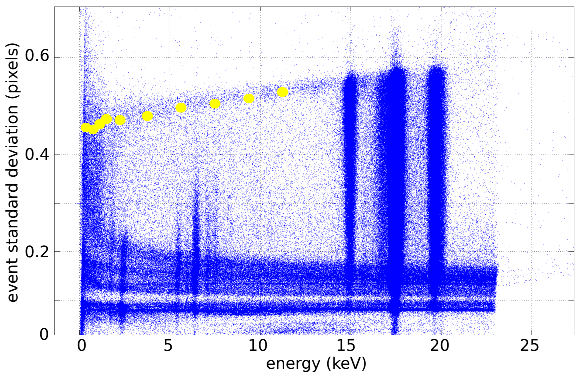

Fig. 5. Standard deviation of the shape of events as a function of their energy. Blue points: measured when a 250 μm-thick CCD is expose to a source of Molybdenum, Yellow points: results from simulation of events interacting at edge of the detector (250 μm).

3) The loop ends when all free charges have reached the edge of the potential Well which was estimated to be at a depth of 10 μ from the gates of the detector, as shown in figure 1.
4) The final position of the charge is used to calculated the standard deviation of the shape of the whole event.

2) Results from simulation: Figure 5 show the measured standard deviation of events as a function of their energy. Only events interacting at the back side of the detector were simulated since the depth of interaction is perfectly know since is equal to the detector thickness (250 μ). The simulation produces a well prediction of the measured shape of the clusters. Some small errors in the standard deviation of simulated events are observed mainly at low energies since the number of simulations of free charge is lower and the reconstructed standard deviation has a bigger error.

VI. Conclusions and Future Work

The importance of modeling point-like events has been pointed out in the context of novel neutrino and dark matter experiments based on CCD technology. This model is crucial to evaluate the efficiency of event selection criteria. The incorporation of the repulsion mechanism by free carriers to the typical diffusion analysis depicts the size change as a function of event energy measured with the CCDs. A quantitative analysis using simulations has been addressed in the work to account the effect of this mechanism.

The measured diffusion of X-ray peaks can be used to evaluate the relationship between shape size and depth of interaction. This calibration will be addressed by authors in the near future. For this analysis the well known exponential distribution of the probability of interaction with depth is used. Then, the results from the simulation presented here can be used to decorrelate the repulsion mechanism from the measured relationship and therefore obtain a calibration of the detector for very low energy events where the repulsion is almost absent. Calibration of the event size versus depth of interaction for energies below 1 keV will play an important role on the CCD experiments for particle detection.

Acknowledgments

This work was done under grant PICT 2013-2128, PICT-2014-1225 and with the BECAR-Fullbright program. Miguel Sofo Haro, Guillermo Fernandez Moroni are supported by CONICET; Eduardo Paolini is supported by Universidad Nacional del Sur and Comision de Investigaciones Cientficas de la provincia de Buenos Aires; Juan Estrada, Gustavo Cancelo and Javier Tiffenberg by Fermilab, and Xavier Bertou by CNEA and CONICET.

References

[1] W. S. Boyle, *Nobel lecture: CCD–An extension of man's view*, *Rev. Mod. Phys.* **82** (Aug, 2010) 2305–2306.
[2] G. E. Smith, *Nobel lecture: The invention and early history of the CCD*, *Rev. Mod. Phys.* **82** (Aug, 2010) 2307–2312.
[3] J. Janesick, *Scientific Charge-coupled Devices*. Press Monographs. Society of Photo Optical, 2001.
[4] S. E. Holland et al., *Fully depleted, back-illuminated charge-coupled devices fabricated on high-resistivity silicon*, *Electron Devices, IEEE Transactions on* **50** (2003) 225–238.
[5] DAMIC Collaboration collaboration, A. Aguilar-Arevalo et al., *Search for low-mass wimps in a 0.6 kg day exposure of the damic experiment at snolab*, *Phys. Rev. D* **94** (Oct, 2016) 082006.
[6] G. Fernandez Moroni et al., *Charge coupled devices for detection of coherent neutrino-nucleus scattering*, *Phys. Rev. D* **91** (Apr, 2015) 072001.
[7] J. Barreto et al., *Direct search for low mass dark matter particles with CCDs*, *Physics Letters B* **711** (2012) 264 – 269.
[8] D. Poenaru et al., *Experimental Techniques in Nuclear Physics*. De Gruyter, 1997.
[9] J. Estrada et al., *CCD testing and characterization for dark energy survey*, *Proc. SPIE* **6269** (2006) 62693K–62693K–15.
[10] J. Estrada et al., *Plasma effect in silicon charge coupled devices (CCDs)*, *Nuclear Instruments and Methods in Physics Research Section A: Accelerators, Spectrometers, Detectors and Associated Equipment* **665** (2011) 90 – 93.
[11] G. F. Moroni et al., *Mathematical model of point events in CCD images*, in *2015 XVI Workshop on Information Processing and Control (RPIC)*, pp. 1–6, Oct, 2015. DOI.
[12] S. Holland et al., *Fully depleted, back-illuminated charge-coupled devices fabricated on high-resistivity silicon*, *IEEE Transactions on Electron Devices* **50** (Jan, 2003) 225–238.
[13] E. Gatti et al., *Dynamics of electrons in drift detectors*, *Nuclear Instruments and Methods in Physics Research Section A: Accelerators, Spectrometers, Detectors and Associated Equipment* **253** (1987) 393–399.
[14] R. Bellwied et al., *Studies of dynamics of electron clouds in star silicon drift detectors*, *Nuclear Instruments and Methods in Physics Research Section A: Accelerators, Spectrometers, Detectors and Associated Equipment* **439** (2000) 507–512.
[15] H. Yousef, *Energy dependent charge spread function in a dedicated synchrotron beam pnCCD detector*. PhD thesis, Ph. D thesis, Universität Siegen, Siegen, Germany, 2011.
[16] A. Castoldi et al., *A 3-d simulation code of electron-hole transport and signal formation with coulomb repulsion and thermal diffusion in 2-d semiconductor detectors*, in *Nuclear Science Symposium and Medical Imaging Conference (NSS/MIC), 2012 IEEE*, pp. 961–967, IEEE, 2012.
[17] T. E. Everhart et al., *Determination of kilovolt electron energy dissipation vs penetration distance in solid materials*, *Journal of Applied Physics* **42** (1971) .
[18] H.-J. Fitting et al., *Electron penetration and energy transfer in solid targets*, *physica status solidi (a)* **43** (1977) 185–190.
[19] D. M. Caughey et al., *Carrier mobilities in silicon empirically related to doping and field*, *Proceedings of the IEEE* **55** (Dec, 1967) 2192–2193.
[20] C. Canali et al., *Drift velocity of electrons and holes and associated anisotropic effects in silicon*, *Journal of Physics and Chemistry of Solids* **32** (1971) 1707 – 1720.
[21] S. A. Schwarz et al., *Semi-empirical equations for electron velocity in silicon: Part ii 8212;mos inversion layer*, *IEEE Transactions on Electron Devices* **30** (Dec, 1983) 1634–1639.